Supplementary Information

Isomer-selective Detection of Hydrogen-Bond Vibrations in the Protonated Water Hexamer

Nadja Heine[1], Matias R. Fagiani[1], Mariana Rossi[1], Torsten Wende[1], Giel Berden[2], Volker Blum[1]*, Knut R. Asmis[1]*

[1]*Fritz-Haber-Institut der Max-Planck Gesellschaft, Faradayweg 4-6,14195 Berlin, Germany.*

[2]*Radboud University Nijmegen, Institute for Molecules and Materials, FELIX facility, Toernooiveld 7, 6525 ED Nijmegen, The Netherlands.*

Computational Details

MP2 numbers presented here were calculated using TURBOMOLE V6.2[1] and QZVPP basis sets. The six internal orbitals were kept frozen, the RI approximation was used, and other settings were kept standard.

Density-functional theory (DFT) simulations were calculated using the PBE exchange-correlation functional corrected with a $C_6[n]/R^6$ term (as proposed in Ref.[2]) in order to account for van der Waals dispersion interactions, which we call PBE+vdW. The calculations were performed with the all-electron, localized basis program package FHI-aims[3]. We used *tight* settings for the numeric atom-centered orbital basis sets and integration grids (see Ref. 3 for further details). Anharmonic IR spectra were calculated according to Ref. 4,

$$I(\omega) \propto \omega^2 \int_0^\infty \mathrm{d}t \langle \boldsymbol{\mu}(t)\boldsymbol{\mu}(0)\rangle \, e^{i\omega t} \quad ,$$

where $\boldsymbol{\mu}$ is the dipole moment of the molecule, obtained as the first moment of the electronic density. The vibrational density of states VDOS and the normal mode projected vibrational density of states PVDOS are defined as,

$$\begin{aligned} \mathrm{VDOS}(\omega) &= \sum_j^N \int \exp(i\omega t)\langle \mathbf{v}_j(t)\cdot\mathbf{v}_j(t_0)\rangle_{t_0} dt, \\ \mathrm{PVDOS}(\omega) &= \int \exp(i\omega t)\langle a^k(t)\, a^k(t_0)\rangle_{t_0} dt, \\ a^k(t) &= \sum_j^N \mathbf{v}_j(t)\cdot\mathbf{u}_j^k, \end{aligned}$$

where $\mathbf{v}_j$ is the velocity on atom *j*, and $\mathbf{u}^k$ is the *k*th normal mode of the molecule (normalized to unity) as obtained from the diagonalization of the mass-weighted hessian.

We observe that the MP2 and PBE+vdW energetics agree well, as shown in Table S1 and S2.

Table S1 | MP2 and PBE+vdW relative energies ΔE, and zero point energy corrected relative energies ΔE_{ZPE}, of the **6Z** and **6E** geometries of $H^+(H_2O)_6$.

Method	System	ΔE (kcal/mol)	ΔE_{ZPE} (kcal/mol)
MP2	**6Z**	0.0	0.0
	6E	-0.3	0.9
PBE+vdW	**6Z**	0.0	0.0
	6E	-0.3	0.5

Table S2 | MP2 and PBE+vdW relative energies ΔE, and zero point energy corrected relative energies ΔE_{ZPE}, of the **6Z**·H_2 and **6E**·H_2 geometries of $H^+(H_2O)_6$·H_2.

Method	System	ΔE (kcal/mol)	ΔE_{ZPE} (kcal/mol)
MP2	**6Z**·H_2	0.0	0.0
	6E·H_2	-0.4	1.0
PBE+vdW	**6Z**·H_2	0.0	0.0
	6E·H_2	-0.4	0.4

In Figure S1, the anharmonic spectra of the **6Z** and **6E** geometries, without H_2 attached, are shown (PBE+vdW functional, microcanonical ensemble, 0.5fs time step, 29 ps of simulation, $\langle T \rangle$=50K). Except for a loss of intensity below 2000 cm^{-1} and the sharp doublet (**6Z**) and triplet (**6E**) around 3500 cm^{-1}, we see no substantial changes with respect to the spectra reported in Figure 2 of the manuscript.

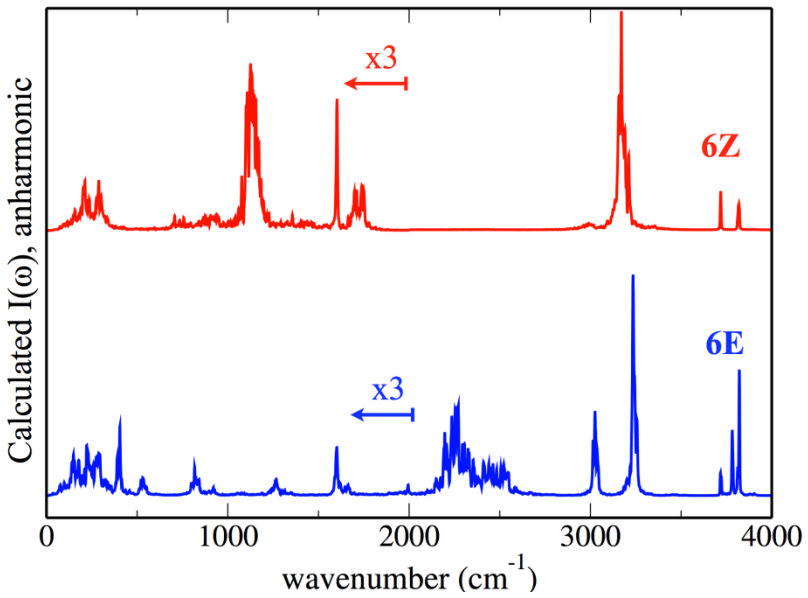

Figure S1 | Calculated anharmonic IR spectra (PBE+vdW, $\langle T \rangle$=50K) of the bare **6Z** and **6E** geometries of $H^+(H_2O)_6$. Below 2000 cm^{-1} the intensities were multiplied by three for better visualization. Spectra are normalized to one for the intensity of the highest peak and are not artificially broadened.

In Figure S2, the harmonic (PBE+vdW) and anharmonic (PBE+vdW, <*T*>=50 K) IR spectra of the **6Z**·H_2 isomer are shown. The anharmonic spectrum is an average over four runs of 10 ps each, starting from different thermalized structures. The statistical error associated with these simulations and the averaging procedure is plotted as a shaded area in Figure S2. We enhance the anharmonic intensities below 1000 cm^{-1} by a factor of five in order to better visualize the low intensity structures between 500 and 1000 cm^{-1}. For this simulation with the PBE+vdW functional, the low intensity structure at ~950 cm^{-1} in the anharmonic spectrum can be attributed to the already present harmonic normal mode at 929 cm^{-1}, that corresponds to a shared proton bend/stretch and the wag of one hydrogen of each internal water molecule (see Figure S3). We observe a coupling of this mode with the shared proton stretch and to the high frequency asymmetric OH stretches from the internal water molecules in a projected VDOS analysis, shown in Figure S3.

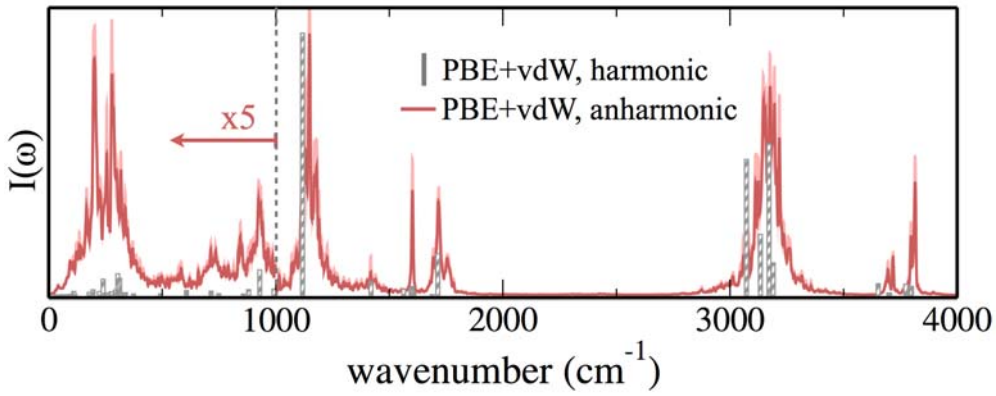

Figure S2 | Calculated harmonic (grey) and anharmonic (red) IR spectra (PBE+vdW, <*T*>=50K) of the **6Z**·H_2 isomer. The anharmonic spectrum is obtained from an average over four AIMD runs of 10 ps each. The light shaded area corresponds to the statistical error (standard deviation divided by the square root of the number of measurements) of the average of the intensities. Below 1000 cm^{-1} the anharmonic intensities were multiplied by five for a better visualization.

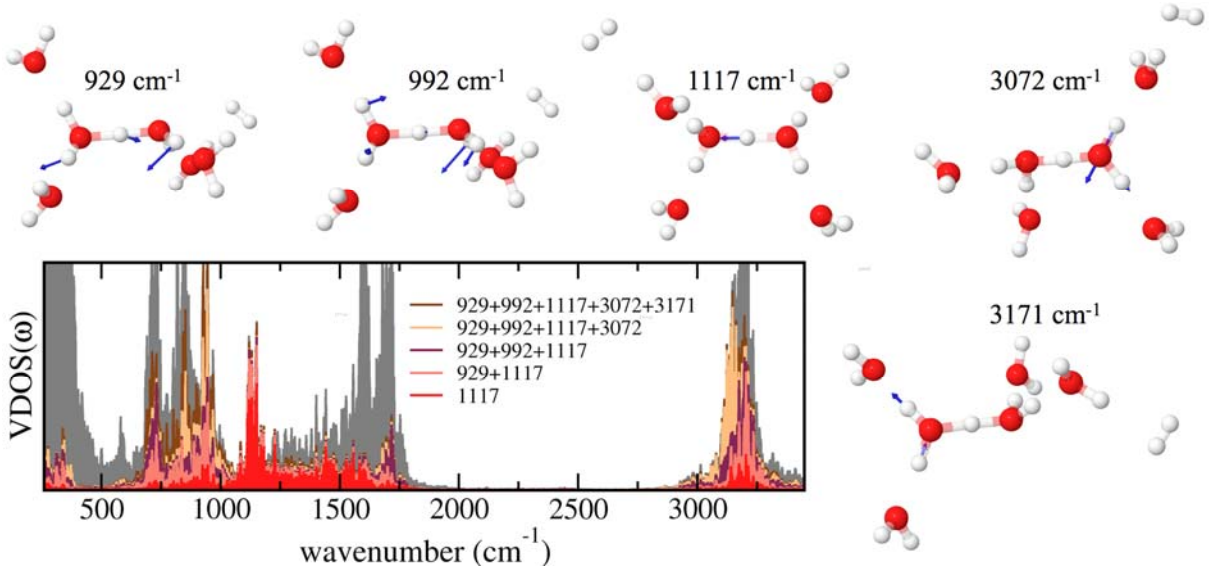

Figure S3 | Full VDOS of the **6Z**·H_2 isomer (grey) calculated from a 20 ps long AIMD PBE+vdW trajectory (<*T*>=50K). In red, salmon, purple, yellow, and brown the sum of the PVDOS in specific normal modes of vibration, labeled in the figure. The peak just below

1000 cm^{-1} owes its full intensity to a coupling between several modes. The vibrations corresponding to the normal modes in question are shown around the plot.

In Table S3 and Figure S4 the harmonic vibrational frequencies and IR intensities for the **6Z**, **6Z**·H_2, **6E**, and **6E**·H_2 geometries are listed and plotted, respectively. The slight differences seen for the tagged and untagged species in the harmonic picture are washed out in the anharmonic cases (see Figures S1 and Figure 3 of the manuscript). Note that six extra modes arise for the H_2-tagged species, so that the frequencies in each line of Table S3 do not directly correspond to one another. Figure S4 shows the complete similarity of the harmonic modes between the untagged and tagged species especially in the shared proton stretch region.

Table S3 | Frequencies and intensities of the harmonic normal modes corresponding to the **6Z**, **6Z**·H_2, **6E**, and **6E**·H_2 geometries, obtained with the PBE+vdW functional (FHI-aims *tight* settings) and not scaled.

6Z		**6Z·H$_2$**		**6E**		**6E·H$_2$**	
Wn. (cm^{-1})	Int. (D^2/Ang^2)	Wn. (cm^{-1})	Int. (D^2/Ang^2)	Wn. (cm^{-1})	Int. (D^2/Ang^2)	Wn. (cm^{-1})	Int. (D^2/Ang^2)
22	0.0	22	0.0	19	0.0	17	0.0
33	0.0	29	0.0	35	0.0	27	0.0
51	0.0	35	0.0	42	0.2	36	0.0
57	0.0	51	0.1	56	0.0	42	0.1
65	0.1	56	0.0	65	0.1	53	0.0
86	0.2	61	0.1	75	0.1	55	0.0
93	0.0	69	0.1	86	0.0	74	0.1
100	0.0	88	0.1	96	0.2	78	0.2
107	0.2	89	0.0	102	0.5	92	0.1
111	1.8	96	0.0	116	1.0	96	0.2
118	0.1	101	0.3	203	4.4	99	0.3
187	0.4	110	1.2	216	3.6	102	0.4
223	0.7	117	0.1	236	1.3	198	2.9
237	8.0	178	0.9	246	1.5	206	2.0
255	2.5	195	1.7	265	1.6	217	4.3
263	1.4	223	1.1	280	1.7	236	0.4
267	0.1	240	5.1	299	4.1	238	1.7
303	6.2	244	0.2	302	1.4	245	1.6
309	5.7	261	0.6	305	0.8	286	0.2
319	0.5	275	1.1	310	2.4	297	1.0
321	0.4	294	1.7	357	0.4	301	3.6
340	1.6	304	6.9	392	1.6	303	0.8
348	0.1	313	5.4	410	3.9	304	0.2
617	0.1	315	0.7	535	1.2	331	3.4
717	1.3	333	0.7	540	1.1	386	1.2
743	0.3	338	0.7	823	0.6	390	1.3
860	0.3	374	0.4	846	2.4	408	3.0
871	2.6	492	0.4	856	2.1	507	0.6
927	11.4	607	1.5	938	1.2	533	1.3
980	1.5	715	1.2	1072	0.6	536	1.0
1098	82.4	749	0.4	1275	3.6	827	1.0
1418	4.3	857	0.3	1578	1.0	844	2.2
1561	1.8	881	1.8	1582	1.1	855	1.7
1595	2.2	929	8.2	1595	0.4	958	1.1
1600	0.2	992	2.0	1613	1.2	1064	0.7
1601	3.0	1118	84.8	1620	0.3	1275	3.6
1607	1.0	1419	4.4	1671	1.1	1579	1.2
1688	0.1	1563	1.8	1689	0.0	1583	1.0
1712	13.0	1596	2.3	2267	107.6	1596	0.2
3134	13.3	1600	0.3	2461	43.4	1614	0.9

6Z		6Z·H$_2$		6E		6E·H$_2$	
Wn. (cm^{-1})	Int. (D^2/Ang^2)	Wn. (cm^{-1})	Int. (D^2/Ang^2)	Wn. (cm^{-1})	Int. (D^2/Ang^2)	Wn. (cm^{-1})	Int. (D^2/Ang^2)
3143	62.8	1601	2.8	3002	32.3	1620	0.3
3143	42.0	1608	0.8	3207	20.1	1674	0.9
3177	3.0	1688	0.1	3214	28.4	1689	0.0
3699	0.7	1713	13.4	3698	0.7	2303	104.9
3699	0.5	3072	44.1	3705	0.6	2483	46.6
3702	0.5	3134	19.7	3706	0.6	2938	32.7
3703	0.6	3172	49.1	3765	1.9	3215	19.3
3794	0.5	3190	10.4	3766	2.3	3222	29.0
3794	4.2	3652	3.7	3792	2.8	3644	3.9
3798	0.7	3699	0.7	3802	2.6	3705	0.6
3798	5.0	3700	0.5	3802	2.7	3706	0.6
		3703	0.5			3765	1.9
		3774	3.5			3766	1.7
		3794	2.1			3766	4.4
		3795	2.8			3802	2.6
		3799	2.8			3803	2.6
		4269	0.3			4267	0.3

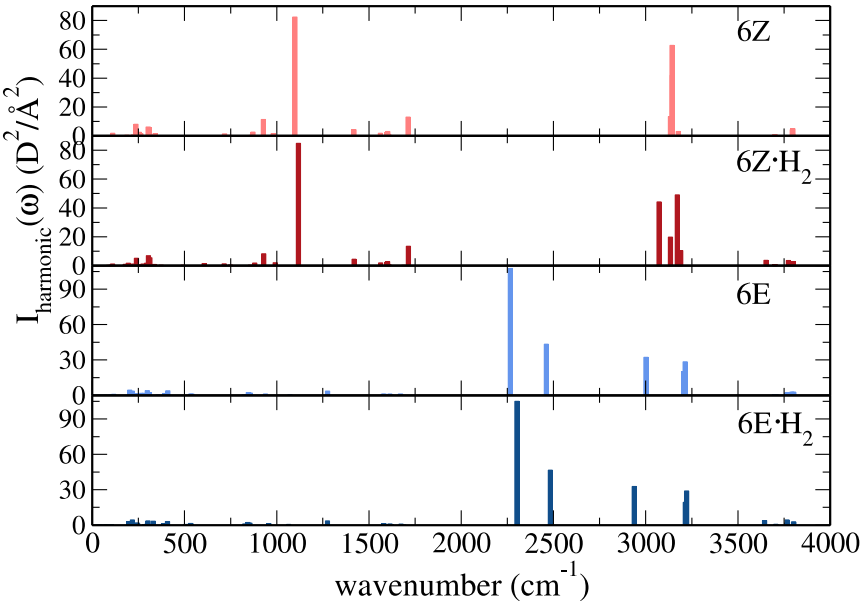

Figure S4 | Visualization of the harmonic frequencies detailed in Table S2 (PBE+vdW, FHI-aims *tight* settings, not scaled).

References

(1) TURBOMOLE V6.2 2010, a development of University of Karlsruhe and Forschungszentrum Karlsruhe GmbH, 1989-2007, TURBOMOLE GmbH, since 2007; available from http://www.turbomole.com.

(2) Tkatchenko, A.; Scheffler, M.; *Phys. Rev. Lett.* **2009**, *102*, 073005.

(3) Blum, V.; Gehrke, R.; Hanke, F.; Havu, P.; Havu, V.; Ren, X.; Reuter, K.; Scheffler, M. *Comput. Phys. Commun.* **2009**, *180*, 2175. http://aims.fhi-berlin.mpg.de/

(4) D. McQuarrie, *Statistical Mechanics*, HarperCollins, 1st Ed., New York, N.Y. (1976).